

# **STUDY OF ENTANGLEMENT IN $\gamma$ -PHOTONS PRODUCED BY PAIR ANNIHILATION USING POCKET GEIGER DETECTORS BASED ON $\gamma - \gamma$ COINCIDENCE METHOD**

*A Report Submitted*  
in Partial Fulfilment of the Requirements  
for the Course

**P443 - Integrated Physics Lab**

*by*  
**Rajdeep Tah (1911124)**



*to the*  
**School of Physical Sciences**  
**National Institute of Science Education and Research**

Bhubaneswar

Date: 13th March, 2023

## ACKNOWLEDGEMENTS

*The successful completion of any task is incomplete and meaningless without giving due credit to the people who made it possible without which the project would not have been successful.*

First and foremost, I am grateful and owe a lot of thanks to my supervisors **Dr. Shovon Pal, Dr. Santosh Babu Gunda** and our Lab Technicians, School of Physical Sciences, National Institute of Science Education and Research, Bhubaneswar for their tremendous support and guidance during the experiment and for providing the proper resources and materials whenever needed. I am also thankful to my lab partner Krishna Kant who was highly supportive and helpful during the entire experiment and helped me a lot with necessary information regarding the same.

Finally, I am thankful to SPS, NISER for giving us such a unique firsthand experience during the integrated masters programme.

## ABSTRACT

In this experiment, we

In this project a theoretical analysis of possibility of obtaining real photons from electron-electron and electron-muon scattering, form one of the most basic form of interactions between leptons with their physical properties described by quantum electrodynamics (QED), in the form of *Bremsstrahlung* radiation. In usual sense, Bremsstrahlung is obtained from the effect of electrostatic potential on an electron scattered by a nucleus. In our case, the effect of electrostatic potential on two electrons or an electron and a muon scattered by each other is analyzed using field theory approach. These are described using three-vertex or four-vertex based tree-level Feynman diagrams. These can be simply considered to be analogous to next or next-to-next order perturbative terms of transition amplitude for original Møller and electron-muon scattering. Finally, we are going to obtain the cross sections of bremsstrahlung process and their angular dependence and finally discuss their significance in comparision with experiments done for the verification of such process to occur.

# Contents

<b>1</b>	<b>Brief Introduction and Theory</b>	<b>1</b>
1.1	The Angular Correlation and Entanglement	3
1.2	Brief Description about Pocket Geiger	3
1.3	Description of the <b>Na-22</b> Source	4
1.4	Mathematical Calculations and Discussions	6
1.5	Real Experimental Setup	7
<b>2</b>	<b>Results and Error Corrections</b>	<b>8</b>
2.1	Data Analysis	8
2.2	Error Analysis	10
<b>3</b>	<b>Discussion and Sources of Error</b>	<b>11</b>
3.1	Outcome of the Experiment	11
3.2	Sources of Error	11
3.3	Our efforts to remove Error	12
	<b>References</b>	<b>13</b>

# List of Figures

1.1	Feynman diagram for Pair Annihilation and $\beta_+$ -decay of <b>Na-22</b> . . . . .	2
1.2	Inelastic Scattering of the $\gamma$ -photon with the Aluminium block. . . . .	3
1.3	Experimental set-up for detecting entangled $\gamma$ -photons. . . . .	4
1.4	Our Experimental set-up for detecting entangled $\gamma$ -photons. . . . .	5
1.5	Characteristics of the Silicon-based Pocket Geiger detector . . . . .	5
1.6	Full Experimental Setup for determining coincidence counts. . . . .	7
2.1	Background Counts for both Detectors. . . . .	8
2.2	Coincidence Counts from the Detectors. . . . .	8
2.3	Coincidence Counts from the Detectors. . . . .	9
2.4	Coincidence Counts from the Detectors. . . . .	9
2.5	Coincidence Counts from the Detectors. . . . .	9

# Chapter 1

## Brief Introduction and Theory

We have learned about the annihilation of a free *electron* ( $e^-$ ) by its anti-particle, i.e. *positron* ( $e^+$ ), to produce a pair of  $\gamma$ -particles which are actually the outcomes of the annihilation radiation generated during this process. The concept of *Pair theory* is a well-established theoretical concept which promotes that two quanta, with *zero* relative angular momentum, emitted during the annihilation of the  $e^- - e^+$  pair, are always perpendicularly polarized with respect to each other. As shown in Fig.(1.1a), the Feynman diagram represents the previously mentioned process. As I mentioned before, we can observe the perpendicular polarization of the emitted  $\gamma$ -photons in the frame where the relative angular momentum is zero i.e. in the Centre of Momentum (COM) frame. This indicates that in the COM frame, we have the two  $\gamma$ -photons emitted in opposite directions with a relative azimuth of  $180^\circ$  and upon a simple calculation of the rest mass energy of the pair of  $\gamma$ -photons, we find that their per photon energy is about  $511 \text{ keV}$ . This shows the Angular correlation of the  $\gamma$ -photons which are generated due to the pair annihilation of the electron and the positron respectively.

Now, we know that we can generate free electrons, as well as positrons, using the  $\beta$ -decays, where the  $\beta_-$ -decay emits an *electron* and an *electron anti-neutrino* whereas the  $\beta_+$ -decay emits a *positron* and an *electron neutrino*. Now, we need to understand that our experiment involves *Compton Scattering* (which I will discuss later on) and it is very important to keep in mind that the two  $\gamma$ -photons emitted during the annihilation process must be from a SLOW moving electron-positron pair. So, to

perform our experiment, we generally take *Sodium-22* (**Na-22**) as our source, which decays via the  $\beta_+$ -decay, emitting a *positron*, along with a metal piece (for our case, it was *Aluminium*) which functions as our *electron* source. By using Aluminium as our source of electrons, we are considering the fact that the drift velocity of the electrons in the Aluminium block is minimal, which in turn allows Compton Scattering. **Na-22** has a half-life of  $\approx 2.6$  years, which is the longest half-life of a Sodium isotope. The flowchart of the  $\beta_+$ -decay of **Na-22**, as well as the Feynman diagram for Pair Annihilation, is given below in Fig.(1.1b):

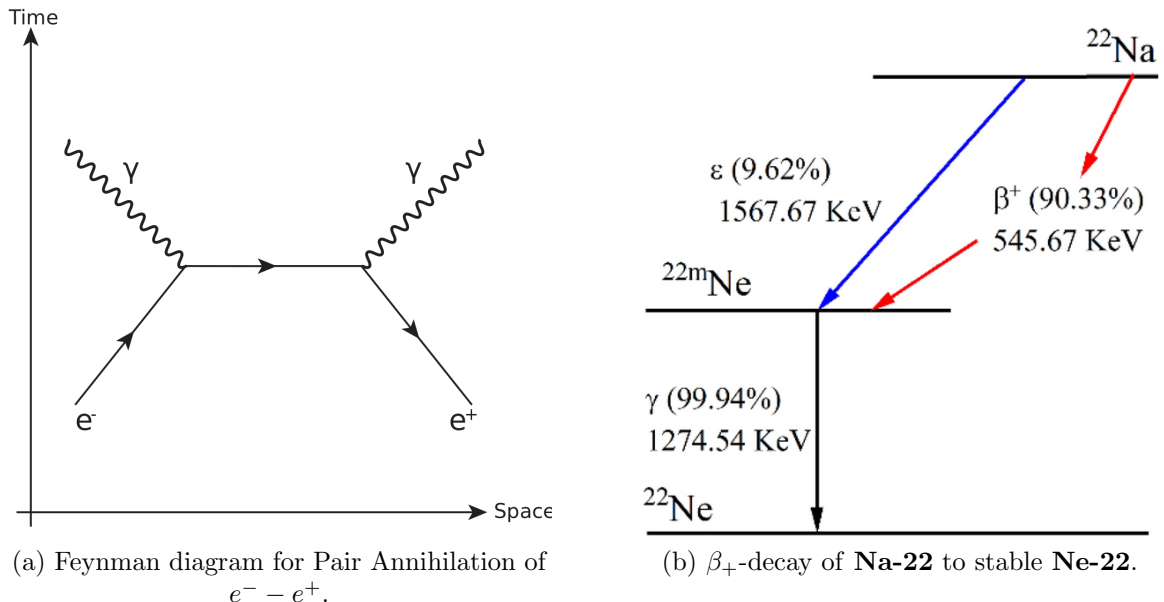


Figure 1.1: Feynman diagram for Pair Annihilation and  $\beta_+$ -decay of **Na-22**

In Fig.(1.1b), we can see that the **Na-22** first decays to **Ne-22** which is in an excited state producing a *positron*, and then, the **Ne-22** gets de-excited by emitting a  $\gamma$ -photon (or radiation) of  $\approx 1274.54$  keV. This whole phenomenon is similar to the one described in the Quantum regime, where their spin is phased out by  $90^\circ$ . These two photons resulting from the annihilation form a single quantum system entangled with another.

## 1.1 The Angular Correlation and Entanglement

In the previous section, I mentioned the Compton Scattering phenomenon in our experiment. We must understand that the Angular polarization of the photons can be determined with the help of Compton Scattering. We use the Aluminium blocks as our Compton Scatterers where the inelastic scattering of the  $\gamma$ -photon takes place with the electron. This leads to the following outcomes: the  $\gamma$ -photon loses its energy after the inelastic scattering and the direction of the outgoing  $\gamma$ -photon changes by an angle  $\theta$ .

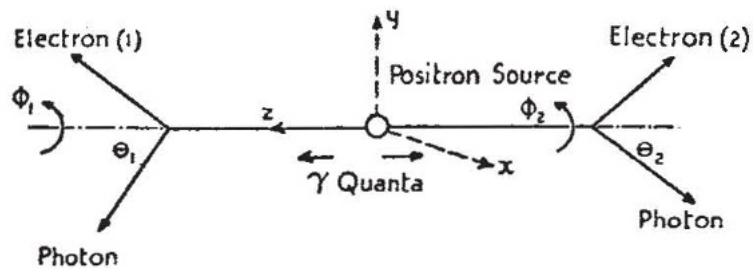


Figure 1.2: Inelastic Scattering of the  $\gamma$ -photon with the Aluminium block.

As we see in Fig.(1.2), if we are able to find the polarization state of one of the  $\gamma$ -photons, then we indirectly know the polarization state of the other, without making any measurement on the other  $\gamma$ -photon. This is called Quantum Entanglement of the two  $\gamma$ -photons produced by the Pair-Absorption. For measuring the counts of the scattered  $\gamma$ -photons, we use the *Pocket Geiger* counter/detector, which works very similarly to the original Geiger counter. Pocket Geigers are mainly made up of Silicon-based semiconductors which are very similar in principle to photo-diodes.

## 1.2 Brief Description about Pocket Geiger

Here, we use the Pocket Geiger detector, mainly made up of Silicon-based semiconductors. We use semiconductors as a base for our detector, and we use it in *reverse*

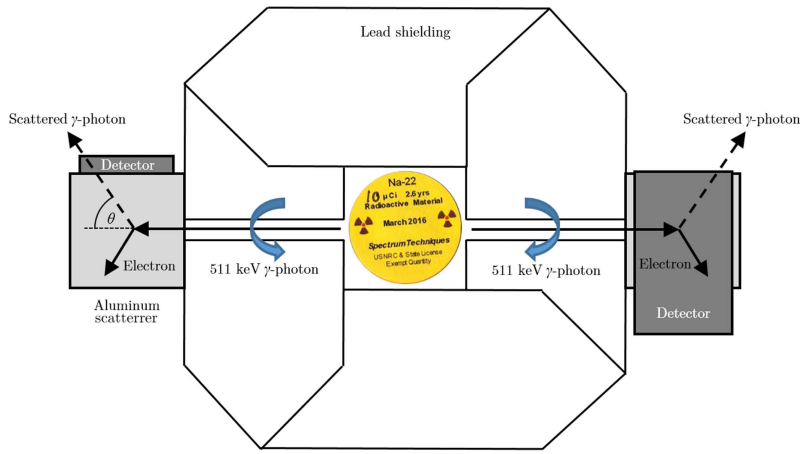


Figure 1.3: Experimental set-up for detecting entangled  $\gamma$ -photons.

*bias* condition since in many cases we find that the thermally generated dark current is much higher than the signal generated by the ionizing radiation. Also, normal GM counters require a very high voltage to operate along with the requirement of a Pulse Shape Analyser at its output. Scintillator detectors also have similar problems, so we use semiconductor detectors. An electric signal in the semiconductor is generated by ionization due to the incident radiation of  $\gamma$ -photons which provides sufficient energy to form electron–hole pairs. Also, Silicon has very high charge carrier mobility ( $\mu$ ) and good mechanical stability which is why we use it as a detector for our experiment.

### 1.3 Description of the Na-22 Source

The **Na-22** *positron* source and a small Aluminium plate are encapsulated in a plastic disk. Positron emitted by the source gets annihilated by the electrons of the aluminium, producing  $\gamma$ -photons which are then detected by the two pocket Geiger detectors. Since the  $\gamma$ -radiation is emitted by a single event, they reach the detectors simultaneously, resulting in a *coincidence* count. Such an experiment which measures the number of coincidences between the two  $\gamma$ -photons obtained from a single event at the source is called a  $\gamma$ - $\gamma$  correlation experiment.

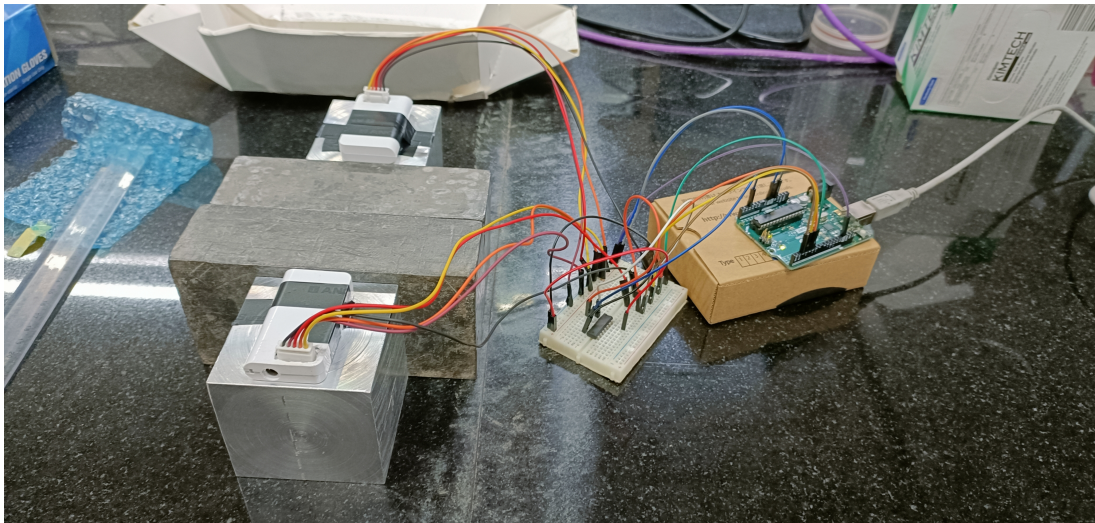
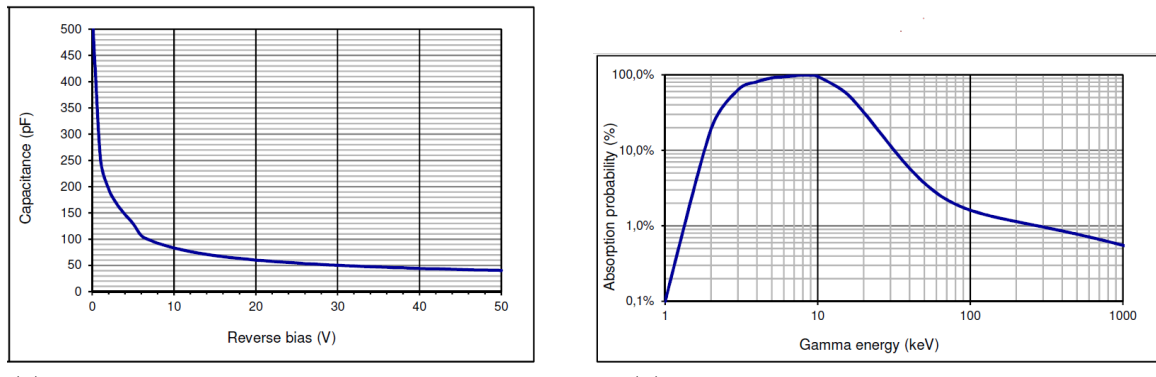


Figure 1.4: Our Experimental set-up for detecting entangled  $\gamma$ -photons.



(a) Plot for Capacitance of the Sensor vs the Applied Reverse bias.

(b) Plot for Efficiency of the Sensor vs the Energy of the  $\gamma$ -photon.

Figure 1.5: Characteristics of the Silicon-based Pocket Geiger detector

From the plots given in Fig.(1.5a) and (1.5b), we can notice that by increasing the Reverse bias, we actually increase the potential barrier which further hinders the charge transfer across the junction. The width of the depletion region increases with increasing reverse bias. Since the depletion region is a volume with an electric field, it can be used as a more sensitive radiation detector.

## 1.4 Mathematical Calculations and Discussions

We have the state of the entangled  $\gamma$ -photons which ensures that the angular correlation manifests itself with different counting rates in relation to the relative position of the detectors. One of the detectors is maintained at a fixed position, while the other is positioned parallel at first and subsequently placed orthogonally with respect to the first one. The two detectors are operated in coincidence mode to detect only the  $\gamma$ -photon pairs generated by the same pair annihilation. The greater count rate is measured when the two detectors are positioned orthogonal and the minimum when they are aligned parallel. In an ideal case scenario, the ratio between the two counting rates should be equal to 2. So, we define the *Asymmetry Counting Ratio (ACR)* as:

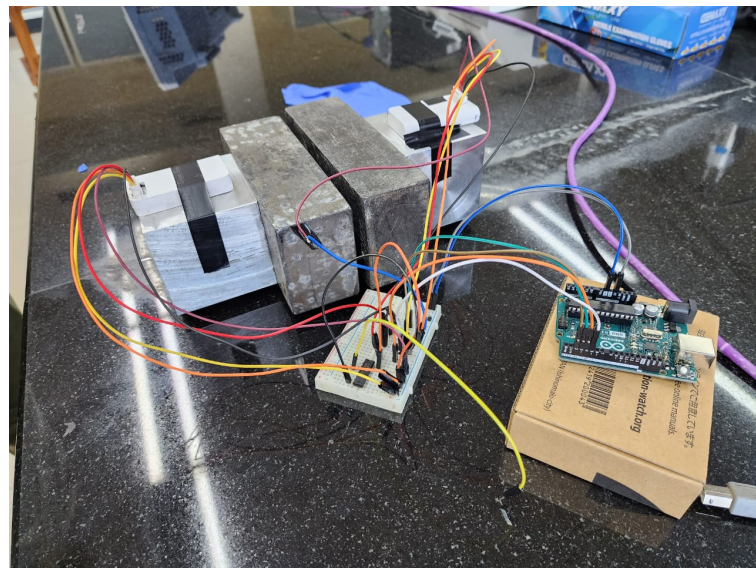
$$\text{ACR} = \frac{\text{Perpendicular Coincidence Counts}}{\text{Parallel Coincidence Counts}} \quad (1.1)$$

As shown in Fig.(1.2) and (1.3), we now have the differential double cross-section ( $d^2\sigma$ ) of the coincident  $\gamma$ -photons which have undergone Compton scattering at angles of  $\theta_1$  and  $\theta_2$  respectively, with the polarization/azimuthal angles at  $\phi_1$  and  $\phi_2$  respectively, is given by:

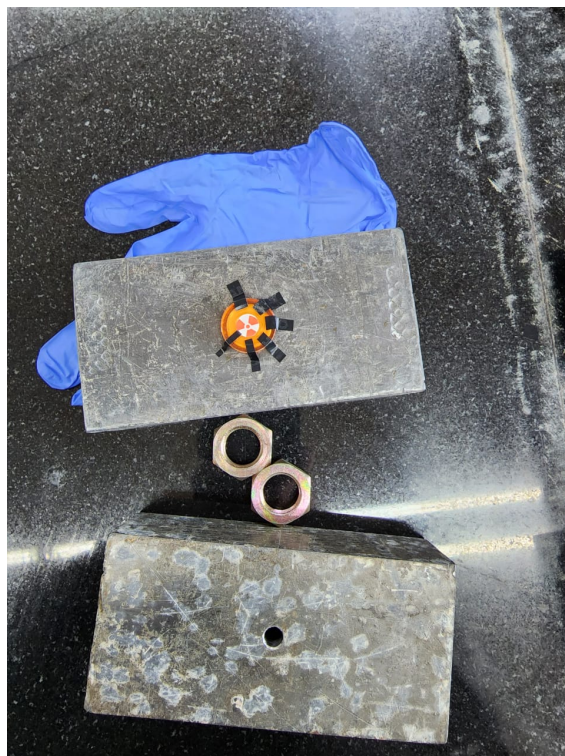
$$\frac{d^2\sigma}{d\Omega_1 d\Omega_2} = \frac{r_0^4}{16} \left[ \frac{\{(1 - \cos \theta_1)^3 + 2\}\{(1 - \cos \theta_2)^3 + 2\}}{(2 - \cos \theta_1)^3(2 - \cos \theta_2)^3} - \frac{\sin^2 \theta_1 \sin^2 \theta_2 \cos 2(\phi_1 - \phi_2)}{(2 - \cos \theta_1)^2(2 - \cos \theta_2)^2} \right] \quad (1.2)$$

where  $r_0$  is the *classical electron radius*, and  $d\Omega_1$  and  $d\Omega_2$  are the differential elements of solid angle for the  $\gamma$ -photons **1** and **2** respectively. Since the second term in the R.H.S only have azimuthal angle dependence, one can see that the expected coincidence rate is maximum for the perpendicular, and minimum for co-planar azimuthal angles of the gamma photons respectively.

## **1.5 Real Experimental Setup**



(a) Experimental Setup with all connections.



(b) **Na-22** source with Lead blocks.

Figure 1.6: Full Experimental Setup for determining coincidence counts.

# Chapter 2

## Results and Error Corrections

### 2.1 Data Analysis

We have the following data for each run of the experiment:

Detector 1		
Background Counts		
20 minutes	113	
Count rate	5.65	cpm
Source Counts (distance = 4.5 cm)		
20 minutes	6809	
Count rate	340.45	cpm

(a) Background Counts for Detector 1

Detector 2		
Background Counts		
20 minutes	107	
Count rate	5.35	cpm
Source Counts (distance = 4.5 cm)		
20 minutes	8806	
Count rate	440.3	cpm

(b) Background Counts for Detector 1.

Figure 2.1: Background Counts for both Detectors.

Coincidence data acquisition 1		
Status: Test		
Lead Collimator Use:	Yes	
Aluminium Scatterer Used:	No	
Time	24	Hours
Coincidence counts	255	

(a) Coincidence Counts in the Absence of the Aluminium Scatterer.

Coincidence data acquisition 2		
Status: Active		
Lead Collimator Use:	YES	
Aluminium Scatterer Used:	YES	
Polarization angle difference	90°	
Time	48	Hours
Count from PG1	18142	
Count from PG2	18169	
Coincidence counts	118	

(b) Coincidence Counts at 90°.

Figure 2.2: Coincidence Counts from the Detectors.

Coincidence data acquisition 3		
Status: Active		
Lead Collimator Use:	YES	
Aluminium Scatterer Used:	YES	
Polarization angle difference	0°	
Time	48	Hours
Count from PG1	18164	
Count from PG2	18235	
Coincidence counts	103	

(a) Coincidence Counts at 0°.

Coincidence data acquisition 4		
Status: Active		
Lead Collimator Use:	YES	
Aluminium Scatterer Used:	YES	
Polarization angle difference	90°	
Time	24	Hours
Count from PG1	17022	
Count from PG2	14777	
Coincidence counts	44	

(b) Coincidence Counts again at 90°.

Figure 2.3: Coincidence Counts from the Detectors.

Coincidence data acquisition 5		
Status: Active		
Lead Collimator Use:	YES	
Aluminium Scatterer Used:	YES	
Polarization angle difference	0°	
Time	24	Hours
Count from PG1	13795	
Count from PG2	14653	
Coincidence counts	29	

(a) Coincidence Counts again at 0°.

Coincidence data acquisition 6		
Status: Active	used NAND gate	
Lead Collimator Use:	YES	
Aluminium Scatterer Used:	YES	
Polarization angle difference	90°	
Time	48	Hours
Count from PG1	31967	
Count from PG2	31847	
Coincidence counts	106	

(b) Coincidence Counts at 90° via the **NAND** gate.

Figure 2.4: Coincidence Counts from the Detectors.

Coincidence data acquisition 7		
Status: Active	used NAND gate	
Lead Collimator Use:	YES	
Aluminium Scatterer Used:	YES	
Polarization angle difference	0°	
Time	48	Hours
Count from PG1	28906	
Count from PG2	29343	
Coincidence counts	106	

(a) Coincidence Counts at 0° via the **NAND** gate.

Coincidence data acquisition 8		
Status: Active		
Lead Collimator Use:	YES	
Aluminium Scatterer Used:	YES	
Polarization angle difference	0°	
Time	24	Hours
Count from PG1	8558	
Count from PG2	7037	
Coincidence counts	12	

(b) Background Coincidence counts of the two detectors.

Figure 2.5: Coincidence Counts from the Detectors.

So, from the acquired data set at Fig.[(2.2b), (2.3a)], Fig.[(2.3b), (2.4a)] and

Fig.[(2.4b), (2.5a)], we have the Asymmetry Counting Ratio (**ACR**) as:

$$ACR_1 = \frac{118}{103} \approx 1.146 \quad (2.1)$$

$$ACR_2 = \frac{44}{29} \approx 1.517 \quad (2.2)$$

$$ACR_3 = \frac{106}{106} = 1 \quad (2.3)$$

where **ACR** is the maximum ratio for the perpendicular polarization counting rate over the parallel polarization counting rate. They are **dependent** on the *Geometry* of the system.

## 2.2 Error Analysis

The measurement error goes as  $\delta = \sqrt{N}$ , where  $N$  is the number of coincidences for each run. So, we have the errors:

$$\text{For first case, } N_{perp} = (118 \pm 10.86) \approx (118 \pm 11) \text{ and } N_{prl} = (103 \pm 10.14) \approx (103 \pm 10) \quad (2.4)$$

$$\text{For second case, } N_{perp} = (44 \pm 6.63) \approx (44 \pm 7) \text{ and } N_{prl} = (29 \pm 5.39) \approx (29 \pm 5) \quad (2.5)$$

$$\text{For third case, } N_{perp} = (106 \pm 10.30) \approx (106 \pm 10) \text{ and } N_{prl} = (106 \pm 10.30) \approx (106 \pm 10) \quad (2.6)$$

So, we have the **ACRs** as:

$$\text{For first case, } ACR_1 = \frac{118 \pm 11}{103 \pm 10} \approx (1.146 \pm 0.047) \quad (2.7)$$

$$\text{For second case, } ACR_2 = \frac{44 \pm 7}{29 \pm 5} \approx (1.517 \pm 0.167) \quad (2.8)$$

$$\text{For third case, } ACR_3 = \frac{106 \pm 10}{106 \pm 10} \approx (1.000 \pm 0.000) \quad (2.9)$$

we can notice that Eq.(2.3) and (2.9) deviate very much from the acceptable value and this might have occurred because of some circuit or data errors.

# Chapter 3

## Discussion and Sources of Error

### 3.1 Outcome of the Experiment

In this experiment, we found that the **ACRs** were within the acceptable range of error for two data sets and this indicates that our experiment was somewhat successful in observing the  $\gamma - \gamma$ -photons entanglement which was generated due to pair annihilation and was detected using the Pocket Geiger detector which worked on the principle of  $\gamma - \gamma$  coincidence. We also found that the counts depended highly on the **arrangement/geometry** of the setup and the materials used as the **Compton Scatterers**. We got very few background counts while taking the coincidence readings and correspondingly deducted them from our observed counts to get accurate counts. Also, we learned about the benefits of using Semiconductor based Detectors over other detectors like the standard GM counter, Scintillation detector etc. We also got yet another exposure to the importance of the functioning of a PN junction in the *reverse bias* mode.

### 3.2 Sources of Error

- The counts might have been disturbed due to fluctuations in the electricity supply since our one experiment ran for a very long time.
- The background counts might have changed over different periods of time and might have introduced some errors in the readings.
- The **Pb** blocks that we have used to prevent outside radiations from interfering

with our experiment (the reason I explained before) might not be the best to prevent all the radiations.

- The geometry of the apparatus matters a lot in this case, and we have seen that it impacts the data obtained. So, this might have also introduced some errors in the data.

### **3.3 Our efforts to remove Error**

- We tried our best not to disturb the setup since the Na-22 source was shielded as much as possible and we ensured that its position didn't change during the experiment.
- We conducted our experiment over a long period of time to ensure we could get the maximum number of coincidence counts and reduce the error in the data.
- We didn't use the **NAND** gate to feed the input signal to the Arduino since it was not working properly which is clearly seen from the data we got while using the NAND gate.

## Reference Journals

1. Jakub Hetfleiš, Jindřich Lněnička and Jan Šlégr, *Entangled  $\gamma$ -photons—classical laboratory exercise with modern detectors* DOI [10.1088/1361-6404/aa8c10](https://doi.org/10.1088/1361-6404/aa8c10).
2. C. S. WU AND I. SHAKNOV, *The Angular Correlation of Scattered Annihilation Radiation* PHYSICAL REVIEW VOLUME: 7, NUMBER 1, JANUARY 1, 1950.
3. M. H. L. PRYCE, J. c. WARD, *Angular Correlation Effects with Annihilation Radiation* No. 4065 September 27, 1947 NATURE.
4. John A. Wheeler, *Polyelectrons* Vol. XLVIII, Art. 3, Annals of the NYAS.